Deterministic Polarimetric Propagation Analysis in Road Tunnels

Esteban Egea-Lopez and Jose-Maria Molina-Garcia-Pardo
Tecnologías de la Información y Comunicaciones
Universidad Politécnica de Cartagena
Cartagena, Spain
esteban.egea@upct.es, josemaria.molina@upct.es

Martine Lienard and Pierre Degauque
IEMN/TELICE
University of Lille
Villeneuve d'Ascq, France
Martine.lienard@univ-lille.fr, pierre.degauque@univ-lille.fr

***Abstract*—The objective of this paper is to study the influence of the direction of polarization at the transmitter site on the characteristics of the propagation channel in a road tunnel, either empty or in presence of vehicles. The transmitting frequency being on the order of 1 GHz, the tunnel behaves as an oversized waveguide and a simulation based on ray propagation is well suited. To take vehicles into account, the ray-based software models vehicles as parallelepiped considering full polarimetric wave interaction. In the examples described in this paper, the polarization at the transmitter is either vertical, horizontal or making an angle of 45°, referred to the horizontal axis. This last orientation that is often practically encountered in mobile communication systems has, to our knowledge, not yet been studied for a road tunnel which strongly differs from urban or suburban areas due to its guiding effect. Path loss, cross-polarization discrimination factor and characteristics of the polarization ellipse at the receiving point are compared for different configurations.**

Keywords- tunnel; propagation; path loss; obstructed tunnel; elliptical polarization.

I. INTRODUCTION

Propagation of high frequency waves in road tunnels, typically in the 1-10 GHz band, has been extensively studied during decades, the theoretical modeling being based generally either on modal or ray theory. Indeed, if the transverse dimensions of the tunnel are much higher than the wavelength, it behaves as an oversized waveguide leading to low longitudinal attenuation.

To improve the performances of the link between vehicle and infrastructure (V2I), or between vehicles (V2V), antenna arrays can be used at both sides of the link [1]. In this case, one of the well-known techniques to increase the channel capacity is based on a Multiple-Input Multiple-Output (MIMO) approach. However, since the propagation of electromagnetic (EM) waves is guided by the tunnel walls, channel diversity could be not high enough so that MIMO could remain efficient in such environment. Theoretical formulations based either on the ray or wave guide theory, as described in [2] and [3] among other papers, have shown that an adequate choice of the antenna array as, for example, the orientation of this array and the element spacing, leads to promising results.

However, the assumption of a straight and empty rectangular tunnel is often used, and one can wonder if, for a tunnel of any shape and in presence of traffic, the characteristics of the link are quite different or not.

In these papers, the polarization of the waves at the transmitter (Tx) is assumed to be generally vertical or sometimes horizontal. However, in practical case, the polarization at a base or relay station is often +/-45°. The objective of this paper is thus to show the possible influence of the polarization on the channel characteristics, which could be due to the geometry of the tunnel behaving as a guided structure and in presence or not of vehicles. For that purpose, a theoretical model of propagation of EM waves in any environment has been developed, as a ray-tracing based propagation simulator which implements the full polarimetric propagation of waves, taking into account plane and curved surfaces, and is able to simulate the presence of vehicles in the tunnel.

The main contributions of this paper are: i) Investigating effect of polarization direction at the transmitter on the propagation channel, ii) characteristics of the polarization ellipse at the receiving point for different configurations and, iii) Influence of vehicles on the channel characteristics.

The paper is organized as follows: The main features of the numerical model are presented in Section II. After a description of the geometrical and electrical parameters used for simulating a 2-lane road tunnel and assuming a frequency of 1.3 GHz, Section III is devoted to the propagation characteristics in an empty tunnel, as path loss, cross-polarization discrimination factor (XPD) and characteristics of the elliptical polarized field at the receiving point (Rx), as tilt angle and axial ratio of the ellipse, which have never been studied. Three directions of linear polarization at Tx are considered: horizontal (H), vertical (V) or inclined (45°). In Section IV, the influence of vehicles is studied, by introducing in the model several trucks, varying from 4 to 20, and distributed on the right lane.

II. RELATED WORKS

A hybrid model applied to a non stationary V2V communication link and taking diffuse reflection into account is proposed in [4]. A modified shooting and bouncing ray (SBR) method and a semi-ellipsoid model to describe the

influence of curved walls of tunnels are detailed in [5] and [6], respectively. Lastly, let us mention that many papers also describe the experimental characterization of the radio channel in tunnel based either on the transmission of an unmodulated carrier at a frequency of 5.8 GHz as in [7], or on a wide band channel sounder whose center frequency is 5.2 GHz [8] or 1.3 GHz [9].

III. Main Features of the Propagation Model

Simulations have been done with Opal [10], a ray-tracing GPU based propagation simulator. Opal is part of the Veneris framework, an open source framework made of a traffic simulator, implemented on top of the Unity game engine and a set of modules which enable bidirectional coupling with the widely used OMNET++ network simulator. Opal uses the shooting and bouncing (SBR) method: electromagnetic waves are simulated by rays launched from the transmitter, either with a given angular separation or with other methods as we will see. These rays are propagated along their trajectory until they hit an obstacle where they are reflected, diffracted, transmitted or scattered. Subsequent rays are traced again. The contributions of the different rays that hit a reception sphere around the receiver are added to compute the electric field. The implementation details can be found in [10].

Opal is designed to handle multiple types of simulation whose execution will be called sequentially. This allows us to combine or disable independent propagation mechanisms at will, such as reflections and diffractions. As propagation mechanisms, Opal currently implements n-order reflections for flat, curved or combined flat-curved scenario elements and single-order diffraction as well as two alternative methods of simulation: (1) a traditional SBR method with duplicate filtering and (2) simulation of n-order reflection for scenes with both curved and flat surfaces that uses the ray density normalization method (RDN) [11]. RDN is a modified SBR method that launches a large number of rays that are uniformly distributed in space. All the rays that hit on the receiver sphere are added and normalized in order to get the correct field contribution. In addition, Opal can compute in parallel the propagation for multiple transmitters and receivers, for moving elements in the scenario, and include antenna patterns for both transmitters and receivers. All the simulations in this paper have been done using the RDN method, with a density of 15.9 million of rays per stereorad.

IV. Propagation in an Empty Tunnel

A. Geometrical and Electrical Configuration

The 2-lane road tunnel is assumed to be straight, of rectangular shape and whose transverse dimensions are 6 m high and 10.2 m width, as shown in Fig. 1a. The conductivity of the walls is 0.01 S/m and their relative permittivity is equal to 5. The frequency is 1.3 GHz.

Tx is situated in the left lane, at a distance of 0.5 m from the nearest wall and at a height of 2.2 m. It is assumed that the Tx antenna has an omnidirectional radiation pattern. Rx moves in the middle of the same lane, the electric field (E) being calculated at a height of 2.7 m. The distance between Tx and

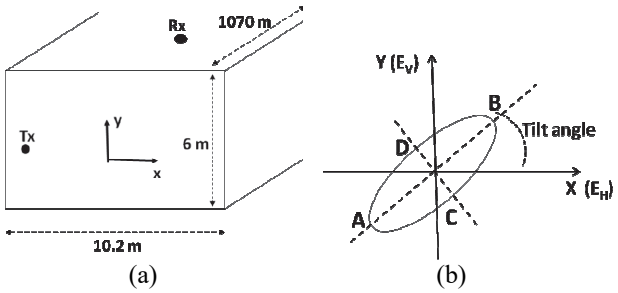

Figure 1. System of coordinates (a) and choice of the reference for characterizing the elliptic polarization at Rx (b).

Rx varies from 63 m up to 1070 m. As already mentioned, the direction of polarization at Tx is either V, H or 45°. At Rx, the polarization of E becomes elliptic due to the multiple reflections on the walls.

The ellipse is characterized, as shown in Fig. 1b, by its tilt angle defined as the angle between its major axis and the horizontal axis, and by its axial ratio, equal to the ratio between the length of the major axis to that of the minor axis (AB/CD).

B. Co-polarization and Cross-polarization Configurations

Curves in Fig. 2 give the relative amplitude of the E field, referred to an arbitrary value, corresponding to a co-polarization (co-polar) configuration, and for 3 directions of polarization at Tx: V, H or 45°. In this case, the component V, H or 45° at Rx are calculated, respectively. To simplify the notation, VV, HH or 45/45 will be used, the first letter referring to the polarization at Tx and the second one the component at Rx.

The global shapes of the 3 curves are quite similar. In this Fig. 2, the dotted lines correspond to the regression line calculated for the different configurations and for a distance greater than 300 m. It thus appears that a simple assumption of an exponential decay can give the per-unit-length average attenuation beyond 300 m.

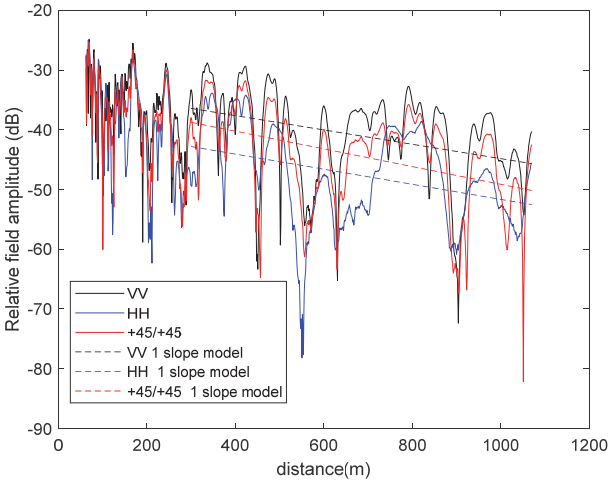

Figure 2. Variation of the field amplitude along the tunnel for a co-polar configuration. Curves for a one-slope model are also plotted.

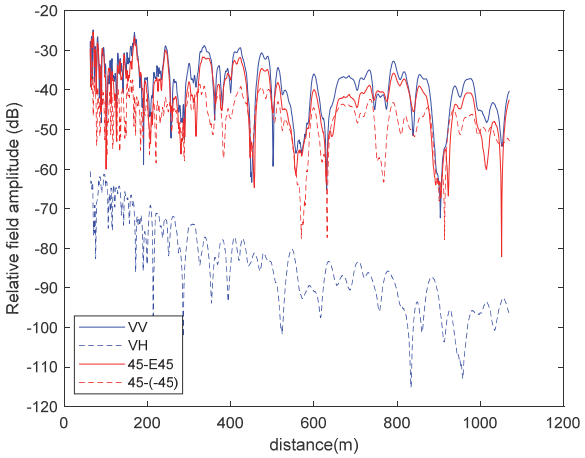

Figure 3. Variation of the field amplitude for copolar (VV or 45-E45) and cross-polar (VH or 45-(-45)) configurations. Polarization at Tx being either vertical (V) or inclined (45°).

Whatever the polarization, path loss is around 1.2 dB/100 m. However, the mean value for VV is higher than that of HH, with a factor of 6.6 dB.

A comparison between the amplitudes of the E components for co-polar or cross-polarization (X-polar) is given in Fig. 3, polarization at Tx site being either V or +45°. If at Tx, the waves are V-polarized, it clearly appears that the VH configuration leads to a strong attenuation. Same result has been obtained for H polarization. On the contrary, for a 45° polarization at Tx, co-polar and X-polar electric field components have the same order of magnitude and XPD, defined as the ratio of their amplitude, can be used to quantify this difference.

C. *Cross-polarization Discrimination Factor*

Variation of XPD versus distance is given in Fig. 4 for V and 45° polarization at Tx. For a V-polarization, XPD is an increasing function of distance, varying from 25 dB at 100 m from Tx, up to 50 dB at 1100 m.

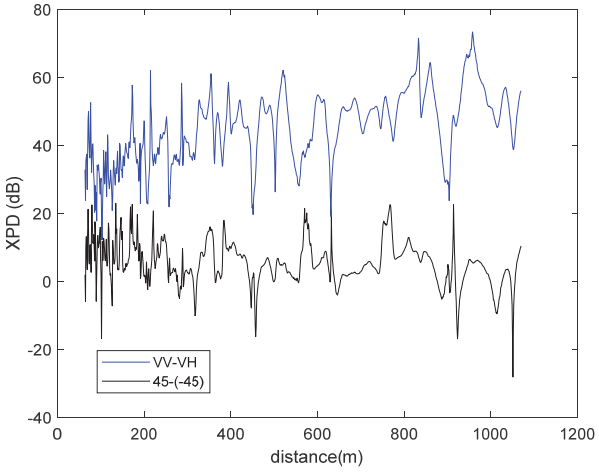

Figure 4. XPD for a V or a 45° polarization at the transmitter

This could be explained by the fact that rays impinging the tunnel walls with a grazing angle of incidence and having nearly the same polarization as at Tx, becomes more and more dominant at large distance. In terms of propagation modes, high order modes giving rise to a X-polar component become less important at large distance.

For explaining results for a polarization at 45°, one can decompose the electric field E at Tx into two in-phase components $E_H(Tx)$ and $E_V(Tx)$ of equal amplitude. At Rx, the E field components are due to the vector addition of the complex fields due to $E_H(Tx)$ on one hand, and to $E_V(Tx)$ on the other hand. However, we have previously seen that XPD is very large if at Tx, waves are V or H polarized. This means that, at Rx, $E_H(Tx)$ leads to only one component $E_H(Rx)$. Similarly, $E_v(Tx)$ leads to $E_v(Rx)$. If $E_H(Rx)$ and $E_v(Rx)$ are in phase, E will be linearly polarized, with a direction of polarization of 45° if these 2 terms have the same amplitude. However, this does not occur since the complex reflection coefficients of the tunnel walls strongly depend on the polarization of the incident wave. Thus $E_H(Rx)$ and $E_v(Rx)$ have neither the same amplitude nor the same phase, giving rise to an elliptic polarization and a strong decrease of XPD.

D. *Cross-polarization Characteristics of the Elliptical Polarization at the Receiver*

From the complex values of two orthogonal components at the receiving point, H and V for example, one can calculate the main characteristics of the ellipse recalled in Section III.a and Fig. 1b. For the 3 linear polarizations at Tx (V, H, 45°), the tilt angle of the ellipse at Rx is shown in Fig. 5.

For H and V polarization, the tilt angle remains nearly constant, equal to about 0° and 90°, the angle being defined with an uncertainty of 180°. This is in agreement with high values of XPD previously outlined. For a 45° polarization, the tilt angle is quite different, mainly varying between 40° and 90°. However, in some cases, the deviation of the tilt angle is more important, and can reach either -40° or 130° at points where deep fading occurs (Fig. 3). For the 45° configuration, the axial ratio is plotted in Fig. 6.

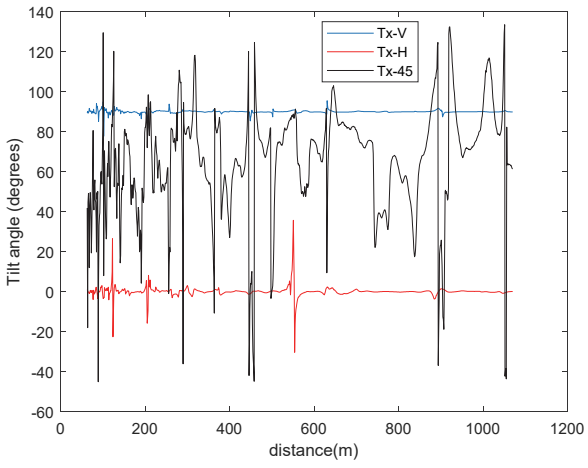

Figure 5. Tilt angle of the ellipse, referred to a horizontal axis

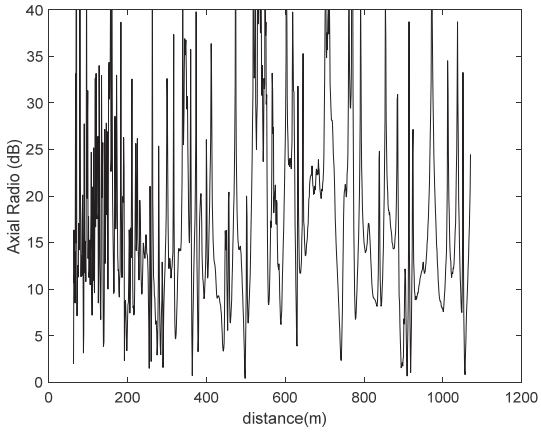

Figure 6. Axial ratio related to the elliptical polarization for a polarization of 45° at the transmitting site.

The fast fluctuations of the curve are due to the fact that, at some point, a deep fading occurs on one field component and not on the other one. The mean value of this ratio is between 15 and 20 dB, meaning that the field approximately remains linearly polarized, but the polarization angle varies with distance, as already shown in Fig. 5.

V. Propagation in Presence of Vehicles

The simulated configuration is given in Fig. 7. Trucks are assumed to be stationary on the right lane of the tunnel, Rx moving on the other lane, free of vehicles. Each truck is modelled by a metallic parallelepiped, its length, width and height being equal to 12 m, 2 m and 4 m, respectively. Since this model is rather rough in terms of representing the real shape of a truck, diffraction by the metallic vertical and horizontal edges is not be taken into account.

Each truck is situated at a distance of 2.2 m from the nearest vertical wall. For this convoy of trucks, the distance between successive trucks is constant, equal to 40 m. This value corresponds to the minimum distance which must be ensured in a tunnel. The first truck is always situated at a distance of 50 m from Tx and the number of trucks in their lane is either 4 or 20.

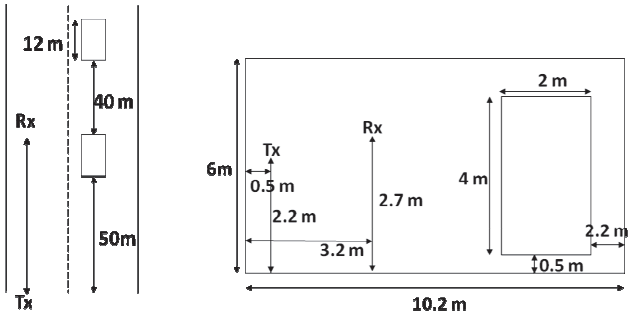

Figure 7. Geometrical configuration of the trucks inside the tunnel

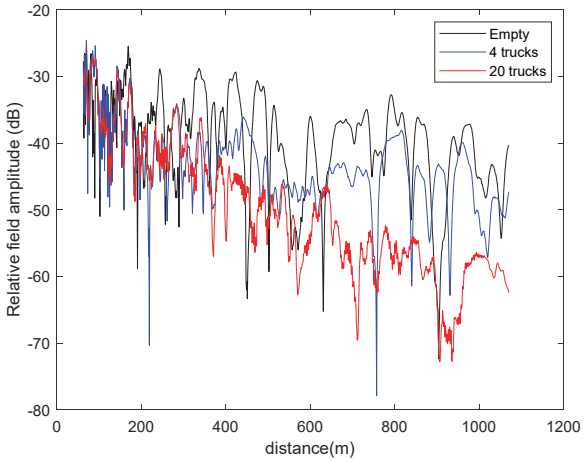

Figure 8. Vertical polarization at Tx. Field amplitude for a co-polar configuration in presence or not of trucks inside the tunnel.

A. *Influence of Trucks on the Amplitude of the Received Field*

Let us first assume a co-polar configuration, the field at Tx being vertically polarized. Curves in Fig. 8 show the relative amplitude of the field if 4 or 20 trucks are situated in a lane, curve for an empty tunnel being also recalled. It appears that the influence of 4 trucks remains small on path loss but when the convoy becomes long enough, with 20 trucks in this example, the field decreases more rapidly. By applying the one-path model, the longitudinal attenuation is of 3 dB/100 m instead of 1.2 dB/100 m for the empty tunnel.

Nearly the same curves were obtained for a H or 45° polarization and are thus not represented. In presence of trucks, the direction of polarization at Tx has no influence on path loss.

B. *Cross polarization Discrimination Factor and Elliptical Polarization at the Receiving Point*

XPD was then calculated for 2 polarizations at Tx: V or 45°, and for a large convoy of 20 trucks. We see in Fig. 9 that waves remain strongly polarized for V polarization, XPD varying from 30 to 60 dB when distance increases. For this configuration the same behavior as that for an empty tunnel is observed.

If the Tx polarization is 45°, XPD is small, and even smaller than in the case of an empty tunnel, XPD being on the order of 5 dB. The tilt angle of the ellipse for V, H and 45° at Tx is given in Fig. 10.

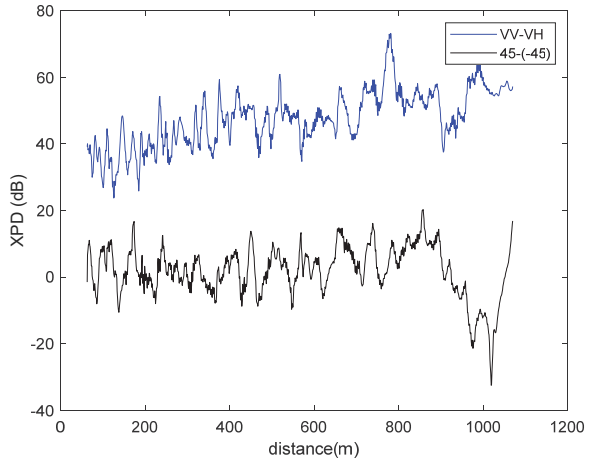

Figure 9. Variation of XPD if the polarization at Tx is either vertical or at 45° and in presence of 40 trucks.

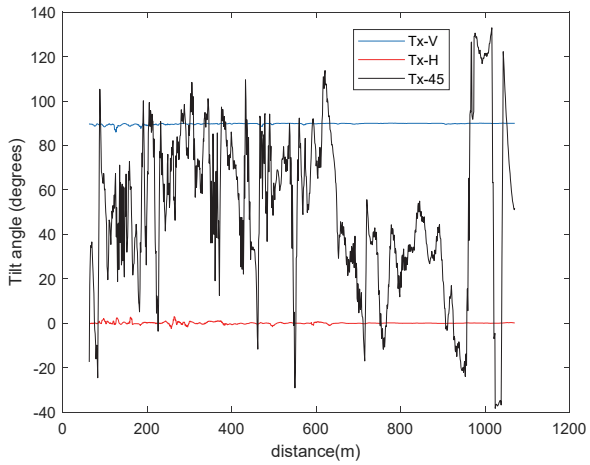

Figure 10. Tilt angle of the ellipse for polarizations at Tx: V, H and 45°.

As in the case of an empty tunnel, the main direction of polarization remains the same as that at Tx, for H and V. For 45°, the tilt angle strongly varies with distance which can be explained by the small value of XPD given in Fig. 9.

It can also be shown that the axial ratio related to the elliptical polarization remains larger than 40 dB for V- or H-polar at Tx. The co-polarized component of the field is dominant and the waves at any receiving point are thus nearly linearly polarized as it happens in an empty tunnel. This axial ratio decreases to 10 - 15 dB for a 45° polarization at Tx, smaller than that for an empty tunnel.

VI. Conclusion

The various examples given in this paper first show that path loss is not strongly dependent on the direction of polarization at Tx, in presence or not of vehicles. However, for other channel characteristics, quite different results are obtained for V-and H-polar at Tx on one hand, and for a 45° polar on the other hand. Indeed, in the first case, the waves remain nearly linearly polarized, the co-polar component at Rx being dominant. In the second case, the direction of the major axis of the polarization ellipse depends on the distance Tx-Rx, and the mean value of the axial ratio of this ellipse becomes equal to 10 -15 dB in presence of vehicles, thus smaller than for an empty tunnel. Similarly, cross polarization discrimination factor for a 45° polar decreases to about 5 dB when vehicles are present in the tunnel. Such a behavior would have an impact on correlation between array elements in multi antenna systems using polarization diversity. Future work will include the simulation taking presence of vehicles on both lanes into account and measurement campaigns at frequencies of 1.3 GHz, as chosen in this paper, but also at 5.9 GHz, dedicated to vehicular communications.

Acknowledgment

This work was supported in part by Grant PID2020-112675RB-C41 (ONOFRE-3) funded by MCIN/AEI/10.13039/501100011033 and Grant PID2019-107885GB-C33. Part of this work was also supported through the ELSAT2020 and RITMEA projects co-financed by the European Union with the European Regional Development Fund, the French state and the Hauts-de-France Region.

References

[1] P. Laly, M. Lienard, P. Degauque, C. Sanchis-Borras, and J. M. Molina-Gracia-Pardo, "Communication in road tunnels: predicted performances of LTE precoding techniques", 5th IEEE Radio and Antenna Days of the Indian Ocean, Proc. pp. 25-28, 2017.

[2] P. Kyritsi and D. Cox, “Expression of MIMO capacity in terms of waveguide modes,” Electron. Lett., vol. 38, no. 18, pp. 1056–1057, 2002

[3] J.-M. Molina-Garcia-Pardo, M. Liénard, P. Degauque, D. Dudley, and L. Juan Llácer, “Interpretation of MIMO channel characteristics in rectangular tunnels from modal theory,” IEEE Trans. Veh. Technol., vol. 57, no. 3, pp. 1974–1979, May 2008.

[4] M. Gan, G. Steinbock, Z. Xu , T. Pedersen, and T. Zemen, "A Hybrid Ray and Graph Model for Simulating Vehicle-to-Vehicle Channels in Tunnels", IEEE Trans. on Vehicular Techno., vol. 67, no 9, pp. 7955-7968, Sept. 2018,

[5] S. H. Chen and S. K. Jeng, "SBR image approach for radio wave propagation in tunnels with and without traffic," *IEEE Transactions on Vehicular Technology*, vol. 45, no. 3, pp. 570-578, Aug. 1996

[6] H. Jiang , Z. Zhang , L. Wu, J. Dang and G. Gui, "A 3-D Non-Stationary Wideband Geometry-Based Channel Model for MIMO Vehicle-to-Vehicle Communications in Tunnel Environments", IEEE Trans. on Vehicular Techno., vol. 68, no 7, pp. 6257-6271, July 2019

[7] A. Santos, L. Matos, P. Castellanos and V. Mota, "Channel Characterization in V2I System inside a Tunnel in 5.8 GHz," SBMO/IEEE MTT-S Int. Microwave and Optoelectronics Conf. (IMOC), pp. 1-3, 2021

[8] J. T. Song, W. Wang, and R. Ibrahim, "The Impact of Obstruction by Vehicle on in-Tunnel Wireless Propagation Channel", pp. 572-576, 2021

[9] M. Yusuf, E. Tanghe, L. Martens, P. Laly, D. P. Gaillot, M. Lienard, P. Degauque, and W. Joseph, "Experimental Investigation of V2I Radio Channel in an Arched Tunnel", 13th European Conf. on Antennas and Propag. (EUCAP), 5 pages, 2019.

[10] Egea-Lopez E, Molina-Garcia-Pardo JM, Lienard M, Degauque P (2021) Opal: An open source ray-tracing propagation simulator for electromagnetic characterization. PLoS ONE 16(11): e0260060. https://doi.org/10.1371/journal.pone.0260060

[11] Didascalou D, Schafer TM, Weinmann F, Wiesbeck W. Ray-density normalization for ray-optical wave propagation modeling in arbitrarily shaped tunnels. IEEE Transactions on Antennas and Propagation. 2000;48(9): 1316–1325.